**Heterogeneous Catalysis** | Hot Paper

Catalytic Co-Conversion of CH₄ and CO₂ Mediated by Rhodium–Titanium Oxide Anions RhTiO₂⁻

Yuan Yang, Ya-Ke Li, Yan-Xia Zhao,* Gong-Ping Wei, Yi Ren, Knut R. Asmis,* and Sheng-Gui He*

Abstract: *Catalytic co-conversion of methane with carbon dioxide to produce syngas ($2\,H_2 + 2\,CO$) involves complicated elementary steps and almost all the elementary reactions are performed at the same high temperature conditions in practical thermocatalysis. Here, we demonstrate by mass spectrometric experiments that $RhTiO_2^-$ promotes the co-conversion of CH_4 and CO_2 to free $2\,H_2 + CO$ and an adsorbed CO (CO_{ads}) at room temperature; the only elementary step that requires the input of external energy is desorption of CO_{ads} from the $RhTiO_2CO^-$ to reform $RhTiO_2^-$. This study not only identifies a promising active species for dry (CO_2) reforming of methane to syngas, but also emphasizes the importance of temperature control over elementary steps in practical catalysis, which may significantly alleviate the carbon deposition originating from the pyrolysis of methane.*

The production of chemical feedstocks from catalytic co-conversion of methane and carbon dioxide, two abundant substances occurring in nature, reduces chemical industry's dependency on traditional fossil fuels and contributes to the

[*] Y. Yang, Dr. Y.-X. Zhao, G.-P. Wei, Y. Ren, Prof. Dr. S.-G. He
State Key Laboratory for Structural Chemistry of Unstable and Stable Species
Institute of Chemistry, Chinese Academy of Sciences
Beijing 100190 (P.R. China)
E-mail: chemzyx@iccas.ac.cn
shengguihe@iccas.ac.cn

Dr. Y.-K. Li, Prof. Dr. K. R. Asmis
Wilhelm-Ostwald Institut für Physikalische und Theoretische Chemie
Universität Leipzig
Linnéstrasse 2, 04103 Leipzig (Germany)
E-mail: knut.asmis@uni-leipzig.de

Y. Yang, G.-P. Wei, Prof. Dr. S.-G. He
University of Chinese Academy of Sciences
Beijing 100049 (P.R. China)

Y. Yang, Dr. Y.-X. Zhao, G.-P. Wei, Prof. Dr. S.-G. He
Beijing National Laboratory for Molecular Sciences and CAS Research/Education Centre of Excellence in Molecular Sciences
Beijing 100190 (P.R. China)

Dr. Y.-K. Li
Fritz-Haber-Institut der Max-Planck-Gesellschaft
Faradayweg 4–6, 14195 Berlin (Germany)

Supporting information and the ORCID identification number(s) for the author(s) of this article can be found under:
https://doi.org/10.1002/anie.202103808.

mitigation of the greenhouse effect.[1] Dry (CO₂) reforming of methane[2] [DRM, reaction (1)] is a potential route to produce

$$CH_4 + CO_2 \rightarrow 2\,CO + 2\,H_2, \quad \Delta H_{298} = +2.56\,\text{eV} \tag{1}$$
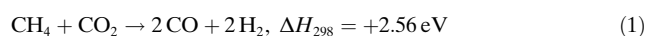
syngas (a mixture of carbon monoxide and hydrogen) that is a crucial feedstock for alcohols, olefins, and Fischer–Tropsch products.[3] However, the inherent stability of both molecules, CH₄ and CO₂, as well as the highly endothermic nature of DRM to syngas requires this thermo-catalysis to be run at high temperatures ($T > 1000$ K), which inevitably leads to coke deposition and catalyst deactivation.[4] Identifying each elementary step of a catalytic cycle offers the possibility to precisely optimize the reaction process and reduce energy consumption. However, catalytic DRM to syngas involves adsorption of CH₄ and CO₂, activation of four C−H bonds to dehydrogenate methane, cleavage of C=O bonds in CO₂, H−H and C_{CH_4}−O_{CO_2} coupling, and desorption of two H₂ and two CO molecules, making it experimentally challenging to follow each of the elementary steps in condensed phase studies.

Gas phase reactivity studies of isolated chemical species that compositionally resemble the local active sites of condensed phase catalysts provide a unique approach to probe the reaction intermediates and understand the molecular-level details of elementary steps involved in the catalytic reactions of practical importance.[5] While a great number of chemical entities (e.g., polyatomic clusters) have been experimentally discovered to activate CH₄[5f–h, 6] or CO₂[5e, 7] under specific reaction conditions, the number of identified species that promote the co-conversion of CH₄ and CO₂ is very limited to date.[8] The atomic cation Ta⁺ is able to co-convert one CH₄ and two CO₂ molecules to H₂ + CO + C₂H₂O at room temperature, but the resulting TaO₂⁺ is difficult to reduce to Ta⁺.[8a] Although catalytic co-conversion of CH₄ and CO₂ was later established over the bimetallic oxide anion RhVO₃⁻, only co-adsorption of CH₄ and CO₂ takes place at room temperature. An increase in the reaction temperature leads to efficient formation of methyl radicals.[8c] Very recently, selective DRM was achieved at room temperature by using Rh₂VO₁₋₃⁻ anions in combination with photo-irradiation to produce the second H₂ and CO molecules.[8d] Herein, we demonstrate that RhTiO₂⁻ co-converts CH₄ and CO₂ to $2\,H_2 + CO$ at room temperature without photo-irradiation. The only elementary step that requires input of external energy to complete the catalytic cycle is the desorption of the second CO molecule.

Figures 1 and S1 show the mass spectra for the reactions of mass-selected RhTiO₂⁻ anions (**1**) with CH₄ and CO₂ in a linear ion trap reactor at room temperature under thermal
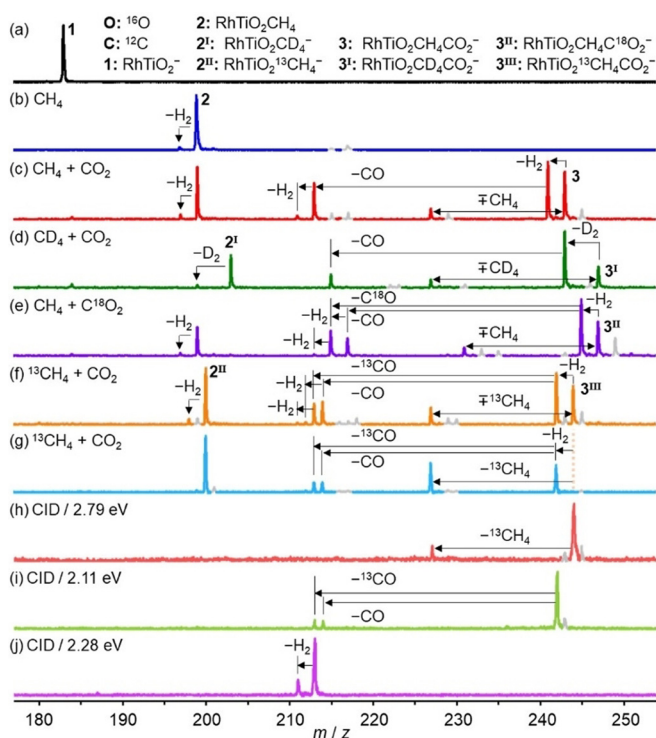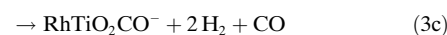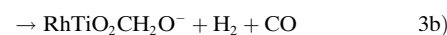
Figure 1. Mass spectra for the reactions of $RhTiO_2^-$ with He (a) and 0.90 Pa CH_4 (b), $RhTiO_2CH_4^-$ with 0.05 Pa CO_2 (c), $RhTiO_2CD_4^-$ with 0.03 Pa CO_2 (d), $RhTiO_2CH_4^-$ with 0.03 Pa $C^{18}O_2$ (e), and $RhTiO_2^{13}CH_4^-$ with 0.03 Pa CO_2 (f) in the single ion trap experiment in which methane and carbon dioxide are delivered into the same ion trap. Panel (g) shows the mass spectrum for the reaction of mass-selected product ion $RhTiO_2^{13}CH_4^-$ with 0.02 Pa CO_2 in the double ion trap experiment in which methane and carbon dioxide are delivered into different ion traps. The arrows show the loss of neutral products from the ionic species or the adsorption of methane onto the ionic species. The reaction times are 1.6 ms for (b,g) and 2.5 ms for (c–f). The spectra for collision-induced dissociation (CID) of $RhTiO_2^{13}CH_4CO_2^-$ (h), $RhTiO_2^{13}CH_2CO_2^-$ (i), and $RhTiO_2CH_2O^-$ (j) generated from the reactions of $RhTiO_2^-$ with $^{13}CH_4/CH_4$ and CO_2 in the same ion trap are shown in the bottom three panels in which the center-of-mass collisional energies are shown.

collision conditions. Upon the interaction with 0.90 Pa CH_4, at first for 1.6 ms, all of the $RhTiO_2^-$ anions were depleted and transformed to the adsorption product $RhTiO_2CH_4^-$ [**2**, Figure 1b and reaction (2a)]. Only very small amounts of $RhTiO_2CH_4^-$ ions are dehydrogenated giving rise to the formation of $RhTiO_2CH_2^-$ (**2**-H_2) + H_2 [reaction (2b)]. The isotopic labeling experiment with CD_4 (Figure S2) confirms the formation of the adsorption product, but the desorption of D_2 molecules did not occur. The pseudo-first (second) order rate constant (k_1) for the reaction of $RhTiO_2^-$ with CH_4 was determined as $(2.2 \pm 0.4) \times 10^{-11}$ $cm^3 s^{-1}$ (Figure S2), corresponding to a reaction efficiency of $(2.2 \pm 0.4)\%$.[9] The kinetic isotopic effect ($k_{1,CH_4}/k_{1,CD_4}$) was estimated to be 1.3 ± 0.2.

$$RhTiO_2^- + CH_4 \rightarrow RhTiO_2CH_4^- \qquad (2a)$$

$$\rightarrow RhTiO_2CH_2^- + H_2 \qquad (2b)$$
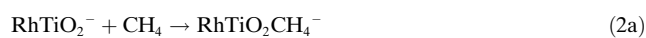
After all of the $RhTiO_2^-$ anions were converted to $RhTiO_2CH_4^-$, CO_2 molecules were pulsed into the ion trap and several new product signals appeared. Figure 1c reveals that in addition to the co-adsorption complex $RhTiO_2CH_4CO_2^-$ (**3**), a strong peak assigned to $RhTiO_2CH_2CO_2^-$ (P1) was observed, corresponding to the loss of the first H_2 molecule [reaction (3a)]. A CO molecule can desorb from P1 to form an appreciable amount of $RhTiO_2CH_2O^-$ ions [P2 = P1−CO, reaction (3b)]. The detection of $RhTiO_2CO^-$ (P3 = P2−H_2) with relatively weak intensity implies that desorption of the second H_2 molecule from P2 [reaction (3c)] is possible, but less efficient. Summarizing, $RhTiO_2^-$ promotes the co-conversion of CH_4 and CO_2 to two free H_2 molecules, one free CO molecule (2 H_2 + CO, syngas) at room temperature. Note that a product peak assigned to $RhTiO_2CO_2^-$ generated from the CH_4/CO_2 exchange was also observed [reaction (3d)]. Isotopic labeling experiments with CD_4 (Figure 1d) confirm the reaction channels (3a)–(3d).

$$RhTiO_2CH_4^- + CO_2 \rightarrow RhTiO_2CH_2CO_2^- + H_2 \qquad (3a)$$

$$\rightarrow RhTiO_2CH_2O^- + H_2 + CO \qquad (3b)$$

$$\rightarrow RhTiO_2CO^- + 2 H_2 + CO \qquad (3c)$$

$$\rightarrow RhTiO_2CO_2^- + CH_4 \qquad (3d)$$

$$RhTiO_2CO_2^- + CH_4 \rightarrow RhTiO_2CH_4CO_2^- \qquad (4)$$

To clarify the O- and C-atom source for CO production, additional isotopic labeling experiments with $C^{18}O_2$ and $^{13}CH_4$ were conducted. Identification of the product ions $RhTi^{16}O_2CH_2^{18}O^-$ and $RhTi^{16}OCH_2^{18}O_2^-$ upon the interaction of $RhTiO_2CH_4^-$ with $C^{18}O_2$ (Figure 1e) shows that the O atom in CO originates from either CO_2 or $RhTiO_2^-$. Next to the product ion $RhTiO_2^{13}CH_2^{12}CO_2^-$, two new signals of $RhTiO_2^{12}CH_2O^-$ and $RhTiO_2^{13}CH_2O^-$ were observed in the reaction of $RhTiO_2^{13}CH_4^-$ with CO_2 (Figure 1f), indicating that both CH_4 and CO_2 can provide a carbon atom for CO generation. Moreover, the weak peaks corresponding to $RhTi^{16}O_2C^{18}O^-$, $RhTiO_2^{12}CO^-$, and $RhTiO_2^{13}CO^-$ in Figure 1e,f confirm desorption of the second H_2 molecule.

In order to confirm the proposed sequential desorption mechanism, we spatially separated the addition of the reactants using two ion trap reactors (instead one). Product ions $RhTiO_2^{13}CH_4^-$ were produced in the first reactor, mass-selected and then interacted with a gas pulse of CO_2 in the second ion trap reactor (Figure 1g). These experiments unambiguously confirm the reactions (3a)–(3d). However, the $RhTiO_2^{13}CH_4CO_2^-$ product was absent, implying that the co-adsorption complexes (**3**, **3**^{I}, **3**^{II}, and **3**^{III}) observed in Figure 1c–f originated from the methane adsorption onto $RhTiO_2CO_2^-/RhTiO_2C^{18}O_2^-$ [reaction (4)]. The CID experiments of mass-selected intermediate complexes $RhTiO_2^{13}CH_4CO_2^-$ (**3**^{III}, Figure 1f), $RhTiO_2^{13}CH_2CO_2^-$ (P1, Figure 1f), and $RhTiO_2CH_2O^-$ (P2, Figure 1c) with Xe were also conducted. The loss of ^{13}CO and CO molecules from P1 and the loss of H_2 from P2 correspond to reaction channels

(3b) and (3c), respectively. The desorption of $^{13}CH_4$ molecule from 3^{III} supports reaction (4).

These experimental results demonstrate that CH_4 and CO_2 are co-converted to $2H_2 + CO$ at room temperature in the presence of $RhTiO_2^-$ and form $RhTiO_2CO^-$ as the product ion. The CID experiments of mass-selected $RhTiO_2CO^-$ with Xe were carried out. When the center-of-mass collisional energy was increased to above 3 eV, the loss of the second CO and regeneration of $RhTiO_2^-$ were observed [Figure S3 and reaction (5)]. Thus, a catalytic cycle involving DRM to syngas [reaction (1)] over $RhTiO_2^-$ was experimentally achieved. Note, no co-conversion was observed when the reaction gases were applied to the ion trap in reverse order, first CO_2 followed by CH_4 (Figures S4 and S5).

$$RhTiO_2CO^- \xrightarrow{CID} RhTiO_2^- + CO \qquad (5)$$

The structure of the $RhTiO_2^-$ anion was characterized by photoelectron spectroscopy (PES) combined with density functional theory (DFT) calculations (Figure S6).[10] The lowest-lying isomer of $RhTiO_2^-$ is a singlet that has a three-membered ring of Rh-Ti-O with a terminal oxygen (O_t) atom connected to Ti. Due to the absence of a reactor coupled with our PES apparatus and the relatively low ion intensities of reaction products, the structures of $RhTiO_2CH_4^-$, $RhTiO_2CH_2CO_2^-$, $RhTiO_2CH_2O^-$, and $RhTiO_2CO^-$ were not experimentally characterized. The possible structures of these ionic speices were computationally determined.

The most favorable pathways for the reactions of $RhTiO_2^-$ with CH_4 and $RhTiO_2CH_4^-$ with CO_2 are shown in Figures 2, S7–S11. Methane binds to the Rh atom of $RhTiO_2^-$ under activation of the first C−H bond by oxidative addition (I1→I2) and formation of the stable intermediate I2. This is followed by the cleavage of the Rh−O bond in I2, H-atom transfer from the Rh atom to the O_t atom (I2→I3), activation of the second C−H bond by the Rh atom and formation of I4, which contains a Rh−H bond, an OH group, and a three-membered Rh-CH_2-Ti ring. Dehydrogenation of I4 to $RhTiO_2CH_2^-$ is not feasible due to high activation energy barriers (1.24–1.28 eV of I4→TS13/TS15 in Figure S7) and the hot I4 is stabilized by collisions with the buffer gas (He), in agreement with the experimental observation that the $RhTiO_2CH_4^-$ mass peak dominates the mass spectrum (Figure 1b).

The reaction of $RhTiO_2CH_4^-$ (I4) with CO_2 commences with the adsorption of CO_2 and its activation involving the formation of a Rh−C bond in the encounter complex I5. Next, one of the C≡O bonds is cleaved (I5→I22 and I23→I6, Figure S8); during this process, the H atom originally bound to Rh transfers to one of the O atoms (I22→I23 and I6→I7 in Figures 2 and S8), resulting in formation of the lowest energy structure, intermediate I7 (Figure S11), which consists of a four-membered O-Rh-CH_2-Ti ring, two (Ti)−OH groups, and a (Rh)−CO moiety. One of the hydroxy H atoms then transfers back to Rh and H_2C−O coupling occurs (I7→I24→ I25 in Figure S8). Subsequently, the Rh−O bond is ruptured, followed by the successive activation of the third and the fourth C−H bond by the Rh atom (I25→I8→I9) and for-
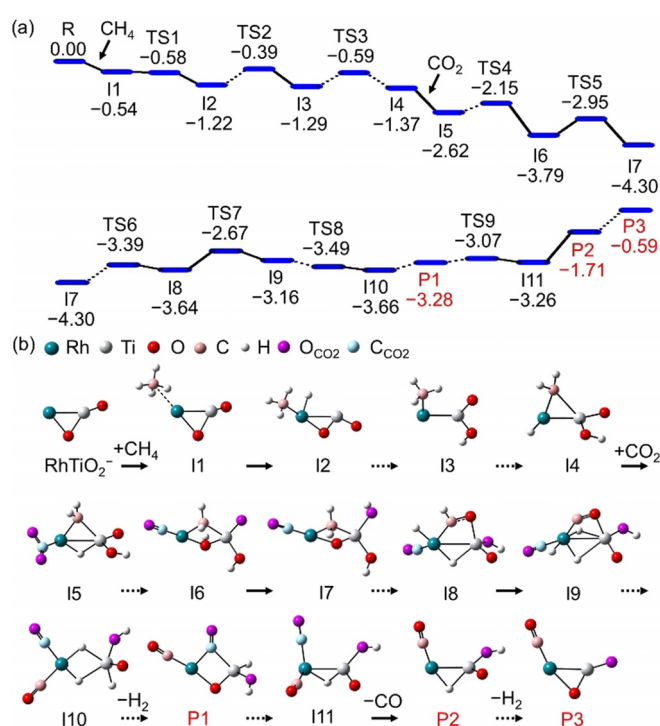

Figure 2. DFT-calculated potential energy profile for the reaction of $RhTiO_2^- + CH_4 + CO_2$ (R) reaction. The zero-point vibration-corrected energies with respect to the separated reactants (ΔH_0) are given in eV. The structures of R, I1–I11, and P1–P3 are plotted and those of TS1–TS9 can be found in the Supporting Information.

mation of I9 containing a Rh-C-O-Ti moiety. After a series of structural rearrangements involving the CO moiety and H-atom transfers (I9→I10), I10, which contains two (Rh)−CO moieties, two bridging and one terminal H atoms, is formed. After several more conversion steps, during which one of the CO moieties in I10 moves towards the Ti atom, molecular hydrogen is formed and evaporated to produce $RhTiO_2CH_2CO_2^-$ (P1, $\Delta H_0 = -3.28$ eV).

P1 still possesses sufficient internal energy to enable desorption of the first CO molecule (P2, $\Delta H_0 = -1.71$ eV) as well as the subsequent desorption of the second H_2 molecule (P3, $\Delta H_0 = -0.59$ eV; in the case that the $RhTiO_2CH_4^-$ is not fully thermalized before reacting with CO_2, the formation of P3 is possible). Note, the reaction course from P1 to P2 involves an important intermediate I11 that contains two equivalent CO moieties, $[C_{CH_4}$-$O_{cluster}]$ and $[C_{CO_2}$−$O_{CO_2}]$, bound to the Rh atom. Either $C_{CH_4}O_{cluster}$ or $(CO)_{CO_2}$ can be desorbed to produce the ionic product $RhTiO_2CH_2O^-$ (P2), consistent with the observed reaction channels in the isotopic labeling experiment (Figure 1). The reaction path for preferential evaporation of the second H_2 molecule from P1 (P1→ $RhTiO_2C_2O_2^- + H_2$, $\Delta H_0 = -2.32$ eV) was also considered. Although it is thermodynamically more favorable than P1→ $RhTiO_2CH_2O^- + CO$, a high energy barrier (1.18 eV of P1→ TS49, in Figure S12) is encountered before H_2 desorption. The rate (4.3×10^8 s^{-1}) of traversing TS49 from P1 was estimated to be two orders of magnitude lower than that for CO evaporation (I11→P2, 1.4×10^{10} s^{-1}) so that CO is preferentially desorbed from P1. The $RhTiO_2C_2O_2^- + H_2$

channel was not observed. After dehydrogenation of $RhTiO_2CH_2O^-$ (P2→P3), the $RhTiO_2CO^-$ ion with CO bound to Rh is formed. Desorption of the second CO to regenerate $RhTiO_2^-$ and close the catalytic cycle of DRM to syngas is overall endothermic by 2.74 eV (Figure S13). This requires supplying additional external energy as shown by the CID experiments. The direct elimination of HCHO and CH_3OH from the reaction of $RhTiO_2CH_4^-$ with CO_2 was also considered. These reaction pathways (Figures S14 and S15) are kinetically less favorable than the H_2 loss channel [reaction (3a)] and ultimately also entropically unfavorable. Therefore, we conclude that the probability for formation of HCHO or CH_3OH is negligible.

Methane conversion has been extensively explored in gas phase studies, which revealed that only a few transition metal-containing oxide ions react with a single CH_4 molecule to generate syngas at room temperature. These are the mono-metallic species $ReO_3^{+[9]}$ and $RuO_3^{+[10]}$ as well as the bimetallic systems $RhAl_3O_4^{+[11]}$ and $RhAl_2O_4^{-}$.[12] However, only a single free H_2 molecule was produced from one CH_4 molecule, because the oxide ions commonly bind the remaining two H atoms in form of two hydroxy groups that are reluctant to liberate H atoms. While the situation is similar in $RhTiO_2^-/CH_4$, i.e., the adsorption complex I4 contains an OH group (Figure 2), which makes H_2 release unfavorable (**2**-H_2 in Figure 1 b). By sharp contrast, the introduction of CO_2 into the reaction system enables the conversion of the four H atoms in CH_4 to two free H_2 molecules at room temperature, greatly enhancing the conversion efficiency of CH_4 to H_2. This work also confirms that by selecting a suitable oxide support (e.g. TiO_2^- cluster), the single Rh atom is sufficiently active to enable the co-conversion of methane with carbon dioxide to syngas, in sharp contrast to the VO_x cluster support, for which the Rh_2 dimer is indispensible for syngas production.[8d]

In condensed phase thermocatalysis of DRM to syngas, methane activation is generally viewed as the rate-determining step and almost all the elementary reactions are performed at the same high temperatures that easily caused pyrolysis of methane (CH_4→C + 2H_2), leading to carbon deposition and catalyst deactivation.[2c] Considerable efforts have been devoted to reduction of carbon deposition by engineering the composition and morphology of catalysts.[4a,c] Our gas phase study on the thermocatalytic DRM to syngas on $RhTiO_2^-$ provides first experimental evidence that both the conversion of CH_4 to $2H_{2,gas} + CO_{gas}/CO_{ads}$ and reduction of CO_2 to CO_{ads}/CO_{gas} can be achievable at room temperature, the only elementary step that requires high temperatures is CO_{ads} desorption (rate-determining step). The insights into the elementary steps of this study should motivate the employment of temperature-programmed methods[13] which could precisely engineer the reaction course of DRM at room or high temperature in practical catalysis. This may significantly alleviate the carbon deposition originating from the pyrolysis of methane.

In conclusion, the co-conversion of CH_4 and CO_2 to syngas mediated by $RhTiO_2^-$ has been achieved in the gas phase. The experimental identification of multiple ionic reaction intermediates confirms that, in principle, the reaction

of $CH_4 + CO_2 \rightarrow 2H_{2,gas} + CO_{gas} + CO_{ads}$ can occur at room temperature. This is also supported by quantum chemical calculations. Only the final step of CO_{ads} desorption requires the input of external energy (e.g., high temperature) to complete the full catalytic cycle. The working conditions for each elementary step of syngas production identified herein underline that the temperature control is very important for optimization of the reaction process and reduction of carbon deposition and energy consumption in practical catalysis.

Acknowledgements

Conflict of interest

The authors declare no conflict of interest.

[1] V. Havran, M. P. Dudukovic, C. S. Lo, *Ind. Eng. Chem. Res.* **2011**, *50*, 7089 – 7100.

[2] a) K. Wittich, M. Kraemer, N. Bottke, S. A. Schunk, *ChemCatChem* **2020**, *12*, 2130 – 2147; b) L. Shi, G. Yang, K. Tao, Y. Yoneyama, Y. Tan, N. Tsubaki, *Acc. Chem. Res.* **2013**, *46*, 1838 – 1847; c) M. A. A. Aziz, H. D. Setiabudi, L. P. Teh, N. H. R. Annuar, A. A. Jalil, *J. Taiwan Inst. Chem. Eng.* **2019**, *101*, 139 – 158.

[3] a) H. M. Torres Galvis, K. P. de Jong, *ACS Catal.* **2013**, *3*, 2130 – 2149; b) A. Galadima, O. Muraza, *J. Nat. Gas Sci. Eng.* **2015**, *25*, 303 – 316; c) H. J. Venvik, J. Yang, *Catal. Today* **2017**, *285*, 135 – 146.

[4] a) M.-S. Fan, A. Z. Abdullah, S. Bhatia, *ChemCatChem* **2009**, *1*, 192 – 208; b) D. Pakhare, J. Spivey, *Chem. Soc. Rev.* **2014**, *43*, 7813 – 7837; c) N. A. K. Aramouni, J. G. Touma, B. Abu Tarboush, J. Zeaiter, M. N. Ahmad, *Renewable Sustainable Energy Rev.* **2018**, *82*, 2570 – 2585.

[5] a) S. Yin, E. R. Bernstein, *Int. J. Mass Spectrom.* **2012**, *321*, 49 – 65; b) Z. Luo, A. W. Castleman, S. N. Khanna, *Chem. Rev.* **2016**, *116*, 14456 – 14492; c) T. Nagata, K. Miyajima, F. Mafuné, *J. Phys. Chem. A* **2016**, *120*, 7624 – 7633; d) M. R. Fagiani, X. Song, S. Debnath, S. Gewinner, W. Schöllkopf, K. R. Asmis, F. A. Bischoff, F. Müller, J. Sauer, *J. Phys. Chem. Lett.* **2017**, *8*, 1272 – 1277; e) L.-X. Jiang, C. Zhao, X.-N. Li, H. Chen, S.-G. He, *Angew. Chem. Int. Ed.* **2017**, *56*, 4187 – 4191; *Angew. Chem.* **2017**, *129*, 4251 – 4255; f) P. B. Armentrout, *Chem. Eur. J.* **2017**, *23*, 10 – 18; g) H.-F. Li, L.-X. Jiang, Y.-X. Zhao, Q.-Y. Liu, T. Zhang, S.-G. He, *Angew. Chem. Int. Ed.* **2018**, *57*, 2662 – 2666; *Angew.*

Chem. **2018**, *130*, 2692–2696; h) Y.-X. Zhao, Z.-Y. Li, Y. Yang, S.-G. He, *Acc. Chem. Res.* **2018**, *51*, 2603–2610; i) Y. Zhao, J.-T. Cui, M. Wang, D. Y. Valdivielso, A. Fielicke, L.-R. Hu, X. Cheng, Q.-Y. Liu, Z.-Y. Li, S.-G. He, J.-B. Ma, *J. Am. Chem. Soc.* **2019**, *141*, 12592–12600; j) H. Z. Ma, A. I. McKay, A. Mravak, M. S. Scholz, J. M. White, R. J. Mulder, E. J. Bieske, V. Bonacic-Koutecky, R. A. J. O'Hair, *Nanoscale* **2019**, *11*, 22880–22889; k) Y.-K. Li, S. Debnath, M. Schlangen, W. Schoellkopf, K. R. Asmis, H. Schwarz, *Angew. Chem. Int. Ed.* **2019**, *58*, 18868–18872; *Angew. Chem.* **2019**, *131*, 19044–19048; l) M. Yamaguchi, Y. F. Zhang, S. Kudoh, K. Koyama, O. V. Lushchikova, J. M. Bakker, F. Mafune, *J. Phys. Chem. Lett.* **2020**, *11*, 4408–4412.

[6] a) C. J. Cassady, S. W. McElvany, *J. Am. Chem. Soc.* **1990**, *112*, 4788–4797; b) U. Achatz, C. Berg, S. Joos, B. S. Fox, M. K. Beyer, G. Niedner-Schatteburg, V. E. Bondybey, *Chem. Phys. Lett.* **2000**, *320*, 53–58; c) G. de Petris, A. Troiani, M. Rosi, G. Angelini, O. Ursini, *Chem. Eur. J.* **2009**, *15*, 4248–4252; d) D. Schröder, *Angew. Chem. Int. Ed.* **2010**, *49*, 850–851; *Angew. Chem.* **2010**, *122*, 862–863; e) S. M. Lang, T. M. Bernhardt, V. Chernyy, J. M. Bakker, R. N. Barnett, U. Landman, *Angew. Chem. Int. Ed.* **2017**, *56*, 13406–13410; *Angew. Chem.* **2017**, *129*, 13591–13595; f) G. Liu, Z. Zhu, S. M. Ciborowski, I. R. Ariyarathna, E. Miliordos, K. H. Bowen, *Angew. Chem. Int. Ed.* **2019**, *58*, 7773–7777; *Angew. Chem.* **2019**, *131*, 7855–7859; g) C. Geng, T. Weiske, J. Li, S. Shaik, H. Schwarz, *J. Am. Chem. Soc.* **2019**, *141*, 599–610; h) N. Levin, J. Lengyel, J. F. Eckhard, M. Tschurl, U. Heiz, *J. Am. Chem. Soc.* **2020**, *142*, 5862–5869.

[7] a) P. Cheng, G. K. Koyanagi, D. K. Böhme, *J. Phys. Chem. A* **2006**, *110*, 12832–12838; b) E. Hossain, D. W. Rothgeb, C. C. Jarrold, *J. Chem. Phys.* **2010**, *133*, 024305; c) A. M. Ricks, A. D. Brathwaite, M. A. Duncan, *J. Phys. Chem. A* **2013**, *117*, 11490–11498; d) G. B. Miller, T. K. Esser, H. Knorke, S. Gewinner, W. Schöllkopf, N. Heine, K. R. Asmis, E. Uggerud, *Angew. Chem. Int. Ed.* **2014**, *53*, 14407–14410; *Angew. Chem.* **2014**, *126*, 14635–14638; e) J. M. Weber, *Int. Rev. Phys. Chem.* **2014**, *33*, 489–519; f) X. Zhang, E. Lim, S. K. Kim, K. H. Bowen, *J. Chem. Phys.* **2015**, *143*, 174305; g) X. Zhang, G. Liu, K.-H. Meiwes-Broer, G. Gantefor, K. Bowen, *Angew. Chem. Int. Ed.* **2016**, *55*, 9644–9647; *Angew. Chem.* **2016**, *128*, 9796–9799; h) H. Schwarz, *Coord. Chem. Rev.* **2017**, *334*, 112–123; i) G. Liu, P. Poths, X. Zhang, Z. Zhu, M. Marshall, M. Blankenhorn, A. N. Alexandrova, K. H. Bowen, *J. Am. Chem. Soc.* **2020**, *142*, 7930–7936.

[8] a) R. Wesendrup, H. Schwarz, *Angew. Chem. Int. Ed. Engl.* **1995**, *34*, 2033–2035; *Angew. Chem.* **1995**, *107*, 2176–2179; b) S. Zhou, J. Li, M. Firouzbakht, M. Schlangen, H. Schwarz, *J. Am. Chem. Soc.* **2017**, *139*, 6169–6176; c) Y. Yang, B. Yang, Y.-X. Zhao, L.-X. Jiang, Z.-Y. Li, Y. Ren, H.-G. Xu, W.-J. Zheng, S.-G. He, *Angew. Chem. Int. Ed.* **2019**, *58*, 17287–17292; *Angew. Chem.* **2019**, *131*, 17447–17452; d) Y.-X. Zhao, B. Yang, H.-F. Li, Y. Zhang, Y. Yang, Q.-Y. Liu, H.-G. Xu, W.-J. Zheng, S.-G. He, *Angew. Chem. Int. Ed.* **2020**, *59*, 21216–21223; *Angew. Chem.* **2020**, *132*, 21402–21409.

[9] M. K. Beyer, C. B. Berg, V. E. Bondybey, *Phys. Chem. Chem. Phys.* **2001**, *3*, 1840–1847.

[10] X. Sun, S. Zhou, L. Yu, M. Schlangen, H. Schwarz, *Chem. Eur. J.* **2019**, *25*, 3550–3559.

[11] Y.-K. Li, Z. Yuan, Y.-X. Zhao, C. Zhao, Q.-Y. Liu, H. Chen, S.-G. He, *J. Am. Chem. Soc.* **2016**, *138*, 12854–12860.

[12] Y.-K. Li, Y.-X. Zhao, S.-G. He, *J. Phys. Chem. A* **2018**, *122*, 3950–3955.

[13] S. C. Fung, C. A. Querini, *J. Catal.* **1992**, *138*, 240–254.